Growth of zinc oxide thin films for optoelectronic application by pulsed laser deposition

K. J. Saji, R. Manoj, R. S. Ajimsha, and M.K. Jayaraj*
Optoelectronic Devices Laboratory, Department of Physics
Cochin University of Science and Technology, Kochi-682 022, India

ABSTRACT

Zinc oxide (ZnO) thin films were deposited on quartz, silicon, and polymer substrates by pulsed laser deposition (PLD) technique at different oxygen partial pressures (0.007 mbar to 0.003 mbar). Polycrystalline ZnO films were obtained at room temperature when the oxygen pressure was between 0.003 mbar and .007 mbar, above and below this pressure the films were amorphous as indicated by the X-ray diffraction (XRD). ZnO films were deposited on Al_2O_3 (0001) at different substrate temperatures varying from 400°C to 600°C and full width half maximum (FWHM) of XRD peak is observed to decrease as substrate temperature increases. The optical band gaps of these films were nearly 3.3 eV. A cylindrical Langmuir probe is used for the investigation of plasma plume arising from the ZnO target. The spatial and temporal variations in electron density and electron temperature are studied. Optical emission spectroscopy is used to identify the different ionic species in the plume. Strong emission lines of neutral Zn, Zn^+ and neutral oxygen are observed. No electronically excited O^+ cations are identified, which is in agreement with previous studies of ZnO plasma plume.

Keywords: Pulsed laser deposition, ZnO thin films, Laser induced spectroscopy, Plasma diagnostics

1. INTRODUCTION

ZnO is a highly interesting and widely studied transparent conducting oxide.[1] The interest in ZnO is fueled and fanned by its prospects in optoelectronics applications owing to its direct wide band gap (*Eg*~3.3 eV at 300 K). Some optoelectronic applications of ZnO overlap with that of GaN, another wide band gap semiconductor (*Eg* ~3.4 eV at 300 K) which is widely used for production of green, blue-ultraviolet, and white light-emitting devices. However, ZnO has the advantage of large exciton binding energy (60 meV). ZnO also has much simpler crystal-growth technology, resulting in a potentially lower cost for ZnO based devices. Recently there has been much interest in the growth of ZnO films for ultraviolet (UV) and blue light emitting device applications. ZnO films generally exhibit n-type conductivity. Conductivity can be improved and stabilized by doping with Al or Ga.[2-4] This property, together with broad optical transparency, has prompted extensive investigations of ZnO films as transparent electrodes in flat-panel displays,[5] thin film transistors[6] and solar cells.[7]

ZnO films have been grown by a variety of methods, including radio-frequency (rf) and direct-current (dc) sputtering,[4,8,9] chemical vapor deposition,[10] spray pyrolysis,[11] electron cyclotron resonance-assisted molecular beam epitaxy,[13] and pulsed laser depositions.[2,13,14]

In contrast to the extensive literature relating to ZnO films produced by pulsed laser deposition (PLD) and their properties, there appears to have been relatively little effort directed towards characterization of the ablation plume from which such films are produced.[15,16] Different mechanisms involved during a laser ablation process are rather complex and the expansion dynamics of the plasma plume, in vacuum or in a background gas are not still fully understood. In the present study we report the pulsed laser deposition of ZnO films on different substrates by PLD and spatial, temporal analysis of ZnO plasma formed during the PLD using a cylindrical Langmuir probe and optical emission spectroscopy (OES). Characterization of the ZnO thin films and analysis of plasma parameters provides information about the dependence of plasma parameters on the quality of films

* mkj@cusat.ac.in; Phone No. +91 484 2577404; Fax No. +91 484 2577595.

Advances in Thin-Film Coatings for Optical Applications III, edited by Michael J. Ellison,
Proc. of SPIE Vol. 6286, 62860D, (2006) · 0277-786X/06/$15 · doi: 10.1117/12.680477

2. METHODOLOGY

Q-switched third harmonic Nd: YAG laser (355 nm) with repetition rate 10 Hz and pulse width of 9 ns was used for the laser assisted film deposition. Laser beam was focused to a spot size 2 mm on the surface of the target and the target was kept in rotation with 23 rotations per minute for uniform ablation. The ZnO films were deposited on quartz, Al_2O_3 (0001), silicon (100) wafer and flexible substrate kapton by ablating sintered ZnO target. These ZnO targets were made by sintering the ZnO powder (99.95 % purity) at 900^{o}C for 5 hours in air to form a 1" diameter target. In the present study, depositions of ZnO films were carried out at room temperature and elevated substrate temperatures. Before starting deposition the deposition chamber was evacuated to a pressure of 10^{-6} mbar. At room temperature the ZnO films on quartz, silicon and kapton (polyimide film) substrates were grown at different oxygen partial pressures varying between 0.007 mbar to 0.003 mbar and at laser energy density of 3 J/cm^2 for 20 minutes resulting film thickness of 200 nm. The target to substrate distance was 4 cm. ZnO films were grown at elevated substrate temperatures 400^{o}C to 600^{o}C on Al_2O_3 (0001) substrates keeping the oxygen pressure during deposition 10^{-4} mbar. Substrate to target distance was kept at 6 cm and deposition was carried out with laser energy density 2 J/cm^2 for one hour. Crystalline nature of the films was confirmed using X-ray diffractometer (Rigaku) using Cu-K_α radiation (1.5414 Å). Thickness was measured using Dektak 6M Stylus profiler. Transmission spectra of the films were recorded using JASCO V 570 UV-VIS-NIR spectrophotometer. The target and chamber are kept at ground potential. In order to study the plasma behavior, the plume emanating from the target surface was focused onto an optic fiber bundle using a spherical lens (f = 50 mm) kept inside the chamber. The other end of the fiber was optically coupled to the entrance slit of a monochromator (Spex 320, Jobin Yvon, 1200 grooves/mm grating, 0.06 nm spectral resolution). Imaging of the spectrum was done by a CCD (Spectrum One 2000, 1024×256 pixels). The spectra of the plume produced by ablating ZnO in vacuum (~10^{-6} mbar) were recorded. The CCD was triggered externally using the Q-switch synchronous voltage pulse from the output of the laser controller.

A cylindrical Langmuir probe having dimensions 200 μm diameter and 5 mm length was introduced into the plasma in a direction perpendicular to the propagation direction of the plasma plume. The probe was biased from –20 V to +20 V and the probe current is derived from digital storage oscilloscope (Tektronix TDS-2014, 100 MHz) signals, which is also triggered using external synchronous pulse voltage from laser source. Measurements were taken from 0.5 cm from the target surface to 4.5 cm.

3. RESULTS AND DISCUSSION

3.1 Structural analysis by XRD

Figure 1 shows the XRD θ – 2θ scan of ZnO thin films grown at room temperature on various substrates and for an oxygen partial pressure of 0.004 mbar. FWHM of the x-ray diffraction peak corresponding to ZnO (002) plane is found to have a minimum value at 0.004 mbar oxygen pressure and after that it is observed to increase with increasing oxygen pressure (Fig.2). Better crystalline films were formed on different substrates at an oxygen background pressure of 0.004 mbar. X-ray diffractograms recorded in the Bragg ω scan mode for the films deposited at temperatures 400^{o}C, 500^{o}C and 600^{o}C are shown in figure 3. FMHM of the rocking curves of films grown at high substrate temperature decreases as the substrate temperature increases and have a minimum value of FWHM 0.8 degree for the sample deposited at 600^{o}C.

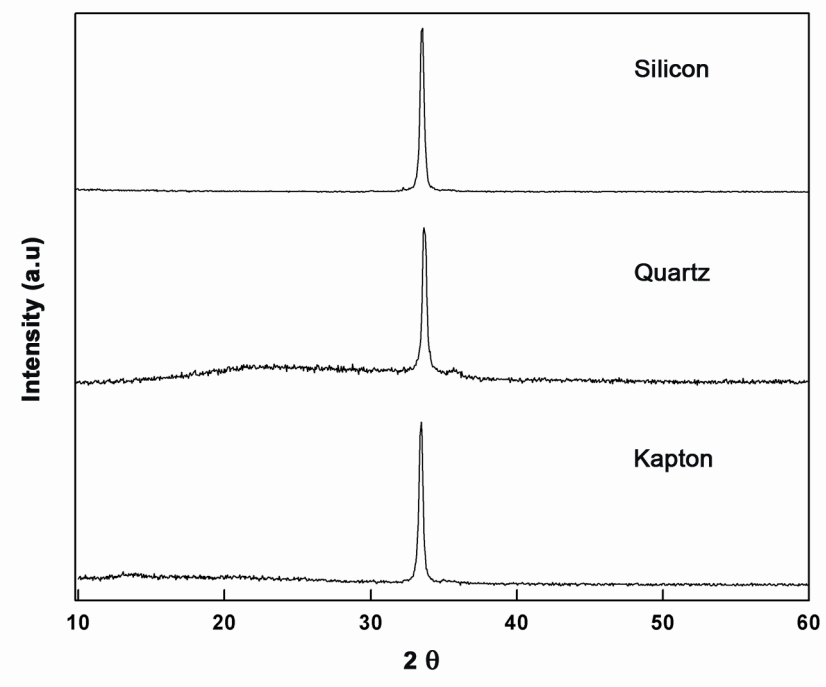

Fig.1. XRD 2θ scan of films deposited on quartz, silicon and plastic substrates at room temperature for 0.004 mbar oxygen partial pressure.

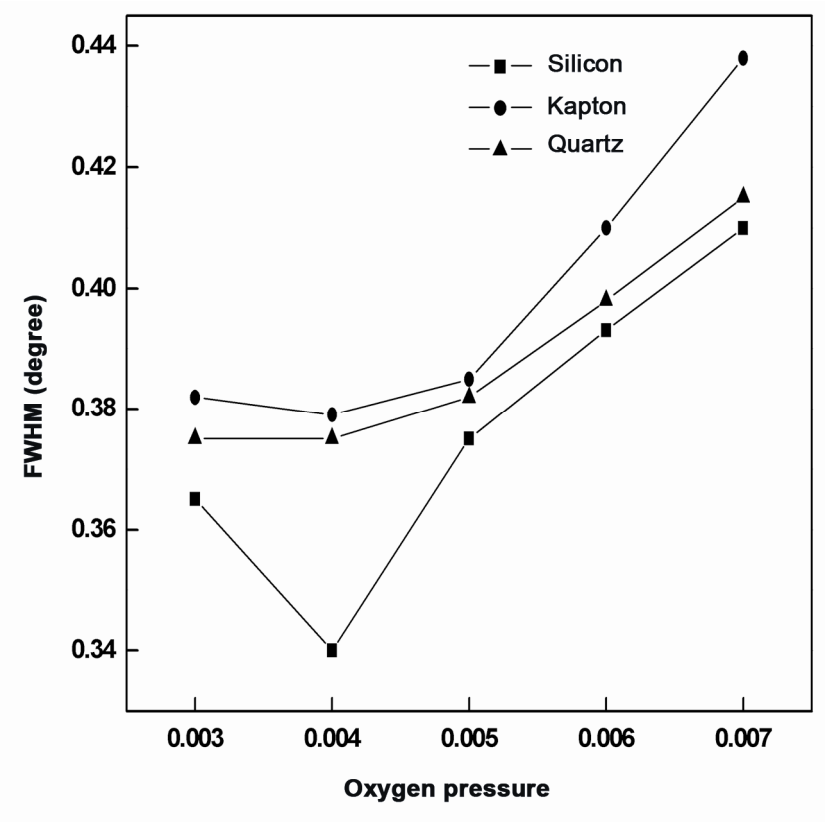

Fig.2. Variations of FWHM of the X-ray diffraction peak corresponding to ZnO (002) plane with increase of oxygen partial pressure

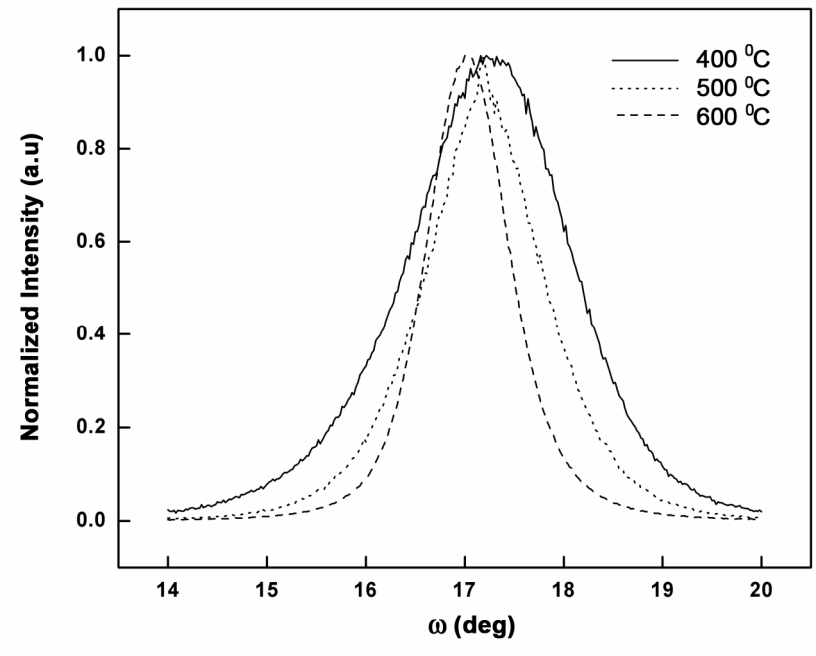

Fig .3. X-ray diffractograms recorded in the Bragg ω scan mode for the samples prepared on Al_2O_3 substrates by varying temperature from 400°C to 600°C

In PLD of ZnO, laser ablated plume containing various ionic species of zinc and oxygen is expanding adiabatically towards the substrate. Kinetic energy of the zinc and oxygen ionic species reaching the substrate is likely to stimulate the motion of the surface and near surface atoms in the deposited film, thereby relieving film stress, and encouraging changes in film morphology and microcrystalline structure. The discussion thus far has implicitly assumed that adatom adsorption and nucleation occurs homogeneously, and at various sites on the substrate surface. Amorphous films with almost uniform thickness were obtained when the deposition was carried out at room temperature at a target to substrate distance of 6 cm. Polycrystalline films of ZnO oriented in the (002) plane having uniform thickness in approximately 1 cm^2 area were formed when the substrate to target distance is decreased to 4 cm. This type of variation in crystalline nature with substrate to target distance was reported by Cherief *et al*.[17] earlier in the case of YCo_5 films grown by pulsed laser deposition. Various ionic species of ZnO in the laser ablated plasma plume bombarding the substrate kept at 4 cm distance from the target surface may have sufficient energy for crystallization in the form of ZnO film. When the substrate is placed at 6 cm the ablated species reaching the substrate may not have the minimum energy required for crystallization and thereby getting amorphous films. Crystalline films were obtained at target to substrate distance of 6 cm, when the substrate temperature was increased, since the ionic species reaching the substrate surface are getting energy needed to crystallize from substrate temperature.

3.2 Thickness variation

The growth rate of ZnO thin film is found to decrease as the substrate temperature increases from 400°C to 700°C (Fig. 4). This reduction in thickness variation is usually expected. The vapor pressure of zinc is high and it increases as substrate temperature increases, resulting in the re-evaporation of the zinc atoms from the substrate before being oxidized.[18,19] The oxygen pressure in the deposition chamber, as mentioned earlier, is kept at 10^{-4} mbar, which may not be sufficient to oxidize the metal atoms or ions reaching the substrate. Above 350°C oxygen also starts to re-evaporate from the substrate surface.

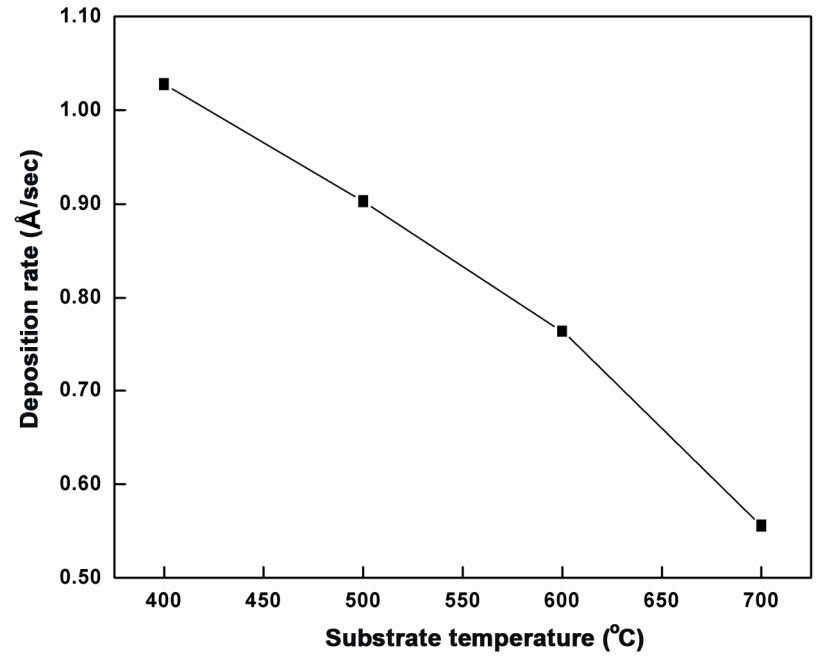

Fig.4. Variation of film deposition rate on Al_2O_3 substrate at different substrate temperatures.

3.3 Optical band gap

Figure 4 shows the transmission spectra of ZnO film deposited on quartz substrate at an oxygen partial pressure of 0.004 mbar. Average transmittance is more than 85% for the samples coated on quartz substrate at different oxygen pressures at room temperature.

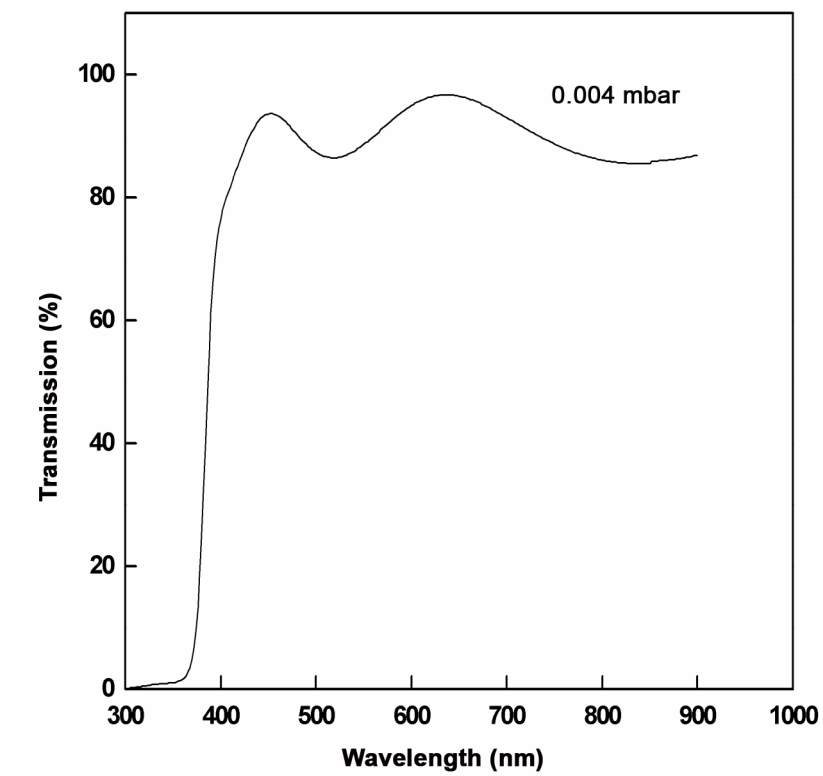

Fig.5. Transmittance spectra of ZnO film deposited on quartz substrate at an oxygen partial pressure of 0.004 mbar.

The optical absorption coefficient α can be calculated from the relation,[20]

$$I = I_0 e^{-\alpha t} \tag{1}$$

where I is the intensity of transmitted light, I_o is the intensity of incident light, t is the thickness of the ZnO films. α near absorption edge is given by

$$\alpha = A\left(h\nu - E_g\right)^n / h\nu \tag{2}$$

Where A is a constant, E_g is the band gap of the material, h is the Planck's constant, ν is the frequency of incident photon and exponent n depends on the type of transition. n may have values 1/2, 2, 3/2 and 3 corresponding to the allowed direct, allowed indirect, forbidden direct and forbidden indirect transitions respectively. The optical band gap was obtained by plotting $(\alpha h\nu)^2$ vs. hν (α is the absorption coefficient and hν the photon energy) and extrapolating the straight-line portion of this plot to the energy axis yields the band gap. Band gap thus obtained varies from 3.26 eV to 3.36 eV for the samples coated on quartz at different oxygen partial pressures varying from 0.007 mbar to 0.003 mbar as shown in figure 5. This variation in band gap can be attributed to Burstein-Moss (BM) shift due to the change in the electron concentration originating from oxygen vacancies which depends on the oxygen partial pressure during deposition.[21]

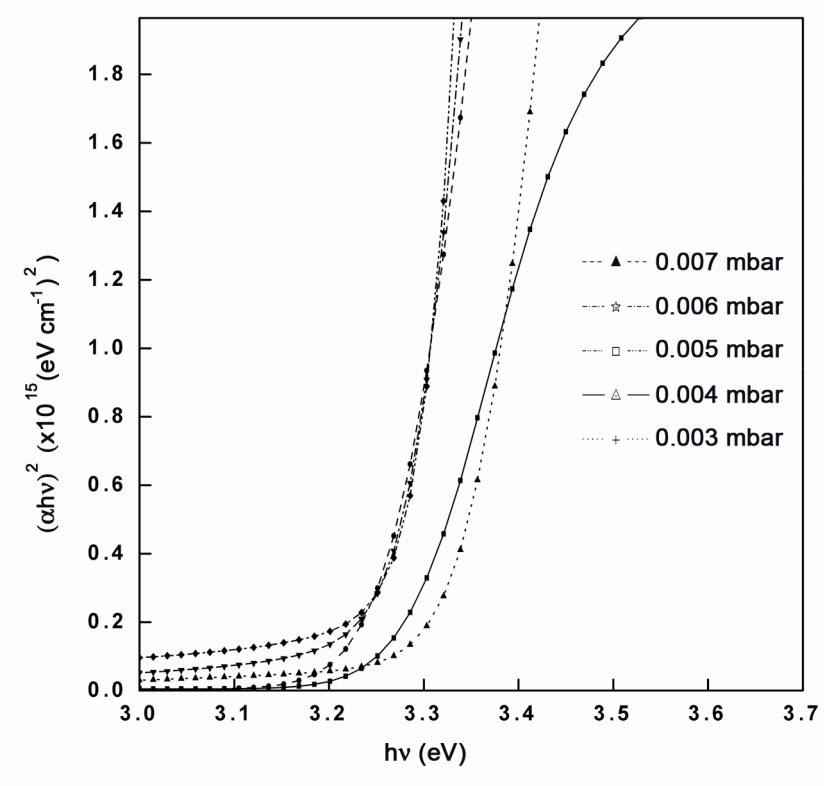

Fig.6. The plot of $(\alpha h\nu)^2$ vs. hν of ZnO films deposited at different oxygen partial pressure. Band gap found to decrease with the increase of oxygen pressure.

3.4 Plasma studies

Plasma represents a heated high-pressure gas kept in a region of small dimensions that later on, is allowed sudden expansion into the surrounding vacuum. In a laser produced plasma the preferential vaporization of the evaporated material is always found to be in a direction perpendicular to the target surface, irrespective of the angle of incidence of laser beam.

The optical emission spectra arising out of the ablation of ZnO were recorded from 400 nm – 850 nm using monochromator and CCD. Strong emission lines of neutral Zn, Zn^+ and neutral oxygen are obtained. Figure 7 shows the wavelength dispersed emission spectra of the plume accompanying the 355 nm pulsed laser ablation (PLA) of the ZnO target in vacuum at a pulse energy of 10 mJ recorded at a distance of 6 mm from the target surface. No electronically excited O^+ cations were identified which is in agreement with previous studies of ZnO plasma.[22]

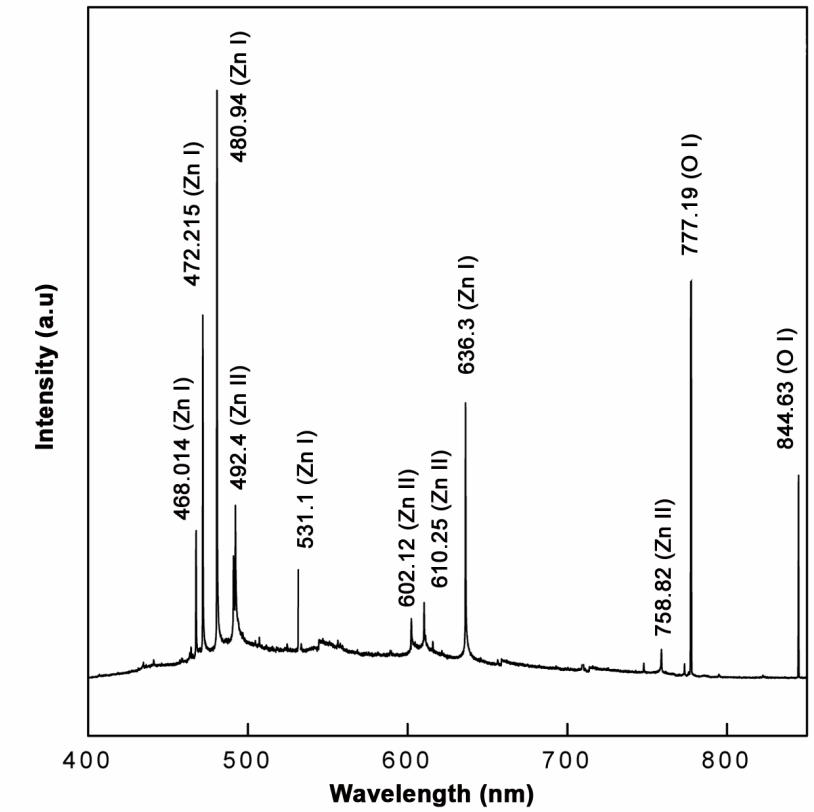

Fig.7. Wavelength dispersed emission spectra of the plume accompanying the 355 nm pulsed laser ablation (PLA) of the ZnO target in vacuum at a pulse energy of 10 mJ recorded at a distance of 6 mm from the target surface.

The plasma arising from PLA is in the local thermodynamic equilibrium (LTE). LTE is said to exist if the time between the collisions of the particle in the plasma is small compared with the duration over which the plasma undergoes any significant change.[23] When electron collisions are the major process of the de-excitation, the system is said to be in LTE. It is clear that LTE will be approached only at sufficiently large particle densities.

According to Langmuir theory, as the probe bias becomes increasingly negative with respect to the plasma potential (V_p), only energetic electrons are collected by the probe. Assuming the electron energy distribution to be Maxwellian, the current drawn by the probe over this region is given by,[24]

$$I_e = I_0 \exp\left(\frac{e(V - V_p)}{kT_e}\right) \tag{3}$$

with

$$I_0 = N_e e A_p \left(\frac{kT_e}{2\pi m_e}\right)^{1/2} \tag{4}$$

Where N_e is the electron number density within the undisturbed plasma and A_p the surface area of the probe. Plotting $ln(I_e)$ against the probe bias voltage V, and taking the gradient over the electron retarding region yields the electron temperature T_e. Substitution of this temperature along with the electron current at the plasma potential (I_o) yields the electron density N_e from equation (4). The plasma potential is determined from the position of the knee in the $ln(I_e)$ *vs. V* curve.

A typical probe signal when the probe is positioned at a distance of 2.5 cm from the target surface and biased at +5 V is shown in figure 8. Two distinct pulses are observed in this plot. Initially there is a very sharp spike with a few ns full

width at half maximum (FWHM) and another one that starts well after the termination of the laser pulse. This second one corresponds to the thermal electrons accompanying the plume. The first spike is resulted from the plasma-induced electric field.[25] The response time of the plasma sheath within the temporally changing plasma environment can be approximated as the reciprocal of the plasma frequency.[26] Here it is found to be of the order of ~50 ps at an electron number density of 10^{17} m^{-3}. This time scale is many orders of magnitude less than the characterizing changes within the current pulse, and hence true plasma environments can be considered sampled by the Langmuir probe.

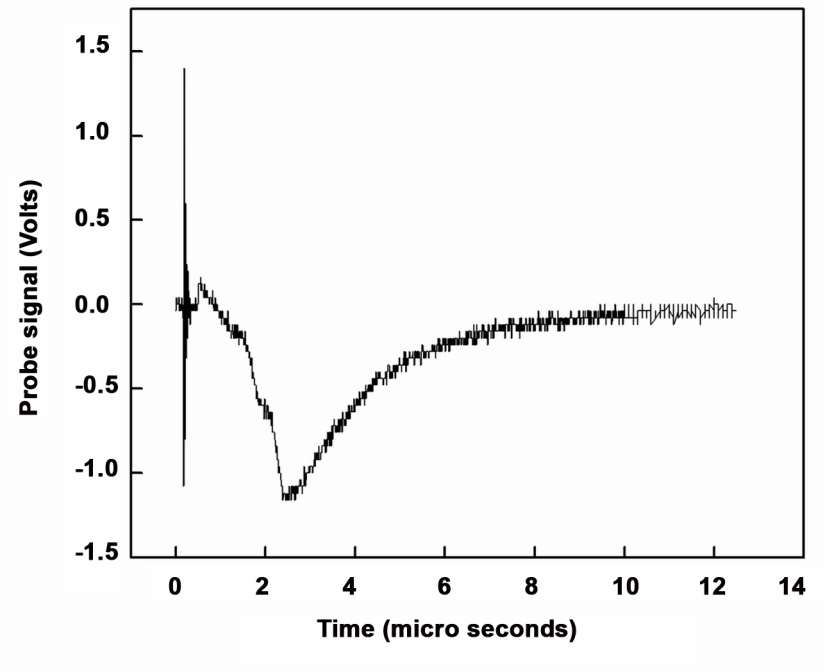

Fig.8. A typical probe signal obtained when the probe is positioned at a distance of 2.5 cm from the target surface and biased at +5 V shows two distinct peaks.

Characteristic current-voltage (I vs. V) curves were constructed from the current verses time (I vs. t) curves, at specific time delays, by taking slices through all the (I/t) data obtained from the digital storage oscilloscope for different probe biases.

The probe signals detected by the digital oscilloscope shows a delay of about 1μs, which indicates that the particles are ejected from the target well after the termination of a laser pulse. The electron number density (Fig.9) increases with time upto around 3 μs and thereafter decreases with time. The small peak in the early stages is caused by the momentary ionization of residual gas in the chamber by the fast moving energetic particles present in the early stage of ablation.[27] Similar peak (Fig .10) is observed at the same instants in the temporal behavior of electron temperature. The electron temperature also increases with time (Fig.10) upto around 2.5 μs and then decreases at the later stages as observed in the ablation of silver by Toftmann *et al*.[28] Depending on time after irradiation, the electron density varies between 0.2×10^{17} m^{-3} to $7.2 \times 10^{17} m^{-3}$ and electron temperature varies between 0.25 eV to 3.3 eV. The electron density decreases almost linearly with distance from the target. A typical plot of N_e at time delays $3\mu s$ and $3.5\mu s$ are shown in figure 11.

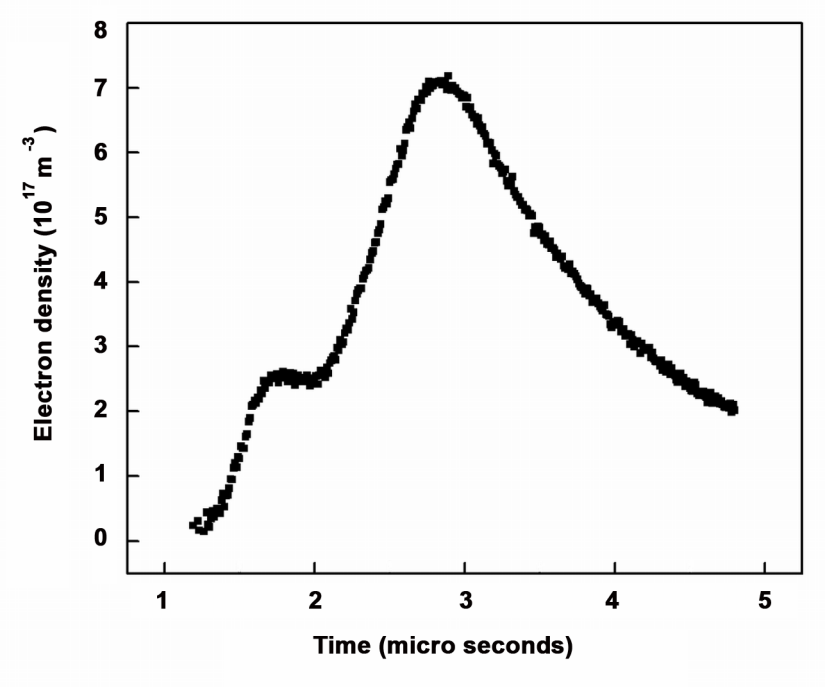

Fig.9. Temporal changes of electron density at a distance of 1.5 cm from the target surface.

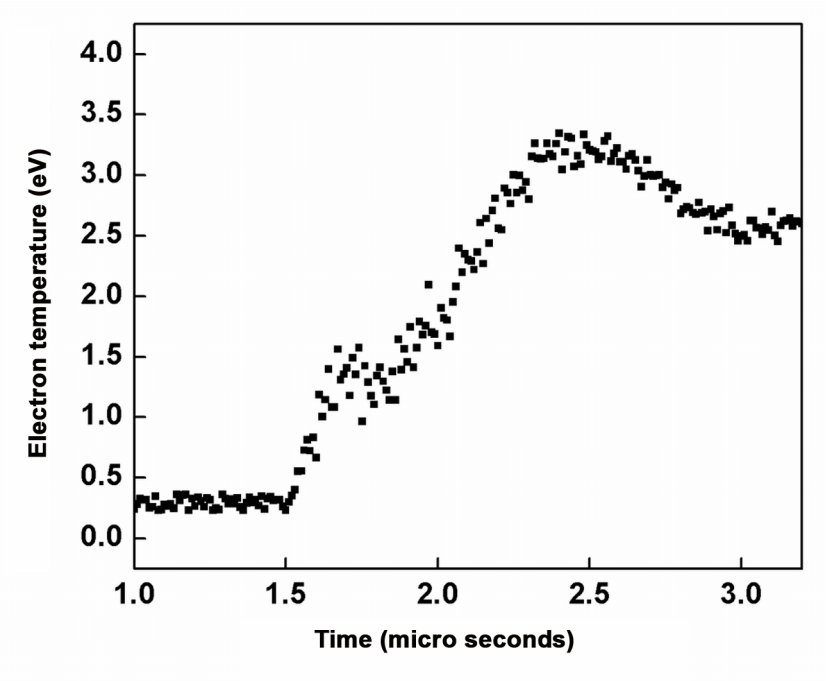

Fig.10. Temporal changes of electron temperature at a distance of 1.5 cm from the target surface.

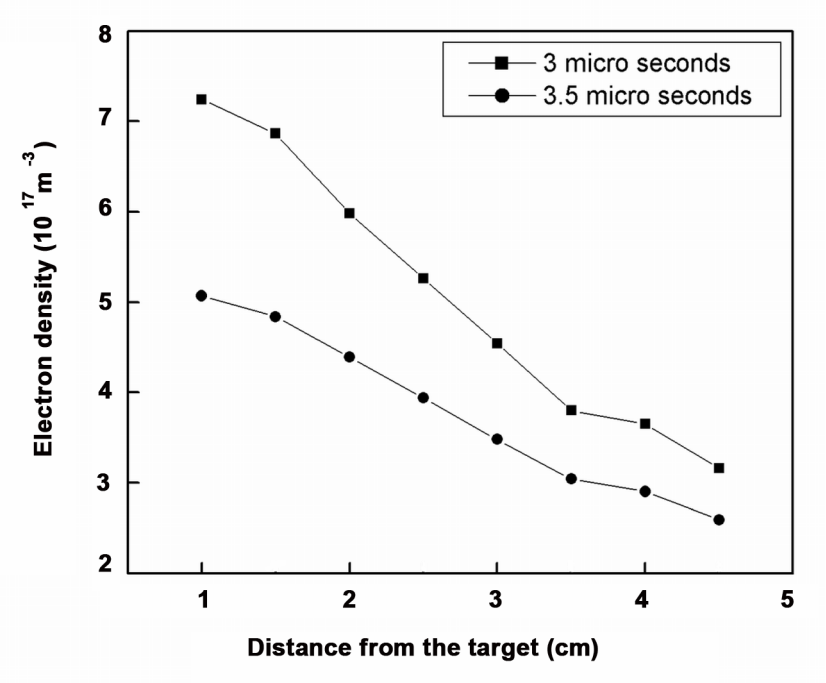

Fig.11. Spatial variations of electron density from the target surface at time delays3μs and 3.5 μs after the laser pulse.

4. CONCLUSION

Deposition conditions are optimized for growth of crystalline zinc oxide films deposited at room temperature by pulsed laser deposition technique. Structural and optical properties of the deposited films are studied. Best crystallinity is obtained when the oxygen partial pressure is 0.004 mbar at a target to substrate distance of 4 cm. Films deposited on single crystalline substrate of Al_2O_3 at 600^oC showed best crystallinity. The band gap of films deposited on quartz exhibited a decreasing tendency with the increase of oxygen partial pressure. Optical emission spectroscopy is used to identify the different ionic species present in the ablated plume. It is observed that particles are ejected from the target well after the termination of a laser pulse. Temporal evolution of electron density and electron temperature are found to follow similar behavior except for a slight difference in the instants for the respective peak values. The peak value of electron density is found to be centered around 3μs after the absorption of a laser pulse. The electron temperature is also found to follow the variations of electron density and is found to have maximum values at around 2.5μs. It is also observed that for a given delay time electron density decreases linearly with the distance from the target.

ACKNOWLEDGMENT

One of the authors (K.J.S) wishes to thank SPIE for travel assistance. The authors thank for the financial supports from Kerala State Council for Science Technology and Environment under SARD program and Department of Science and Technology under FIST program.

REFERENCES

1. Y.Ryu, S. Zhu, D.C.Look, J.M. Wrobel, H.M.Jeong, and H.W.White, "Synthesis of p-type ZnO films" *J. Cryst. Growth* 216(1), 330-334(2000).
2. D. C. Look, D. C. Reynolds, C. W. Litton, R. L. Jones, D. B. Eason, and G. Cantwell, "Characterization of homoepitaxial p-type ZnO grown by molecular beam epitaxy", *Appl. Phys. Lett.* 81(10), 1830 (2002).
3. M.Hiramatsu, K.Imaeda, N.Horio, and M.Nawata, "Transparent conducting ZnO thin films prepared by XeCl excimer laser ablation", *J.Vac.Sci.Technol. A*.16 (2), 669-673 (1998).
4. H.Kim, C.M.Gilmore, J.S.Horwitz,A.Pique, H.Murata, G.P.Kuhsto, R.Schlaf, Z.H.Kafafi, and D.B.Chrisey, "Transparent conducting aluminum-doped zinc oxide thin films for organic light-emitting devices", *Appl. Phys. Lett*.76(3), 259-261 (2000).

5. C. J. Lee, T. J. Lee, S. C. Lyu, Y. Zhang, H. Ruh and H. J. Lee, "Field emission from well-aligned zinc oxide nanowires grown at low temperature", *Appl. Phys. Lett.* 81(19), 3648-3650 (2002).
6. R. L. Hoffman, B. J. Norris and J. F. Wager, "ZnO-based transparent thin-film transistors", *Appl. Phys. Lett*. 82(5), 733-735(2003).
7. Aranovich, Julio, Ortiz, Armando, Bube, and H. Richard, "Optical and electrical properties of ZnO films prepared by spray pyrolysis for solar cell applications", *J. Vacc. Sci. Technol*. 16(4), 994-1003 (1979).
8. B. Lin, Z. Fu, and Y. Jia, "Green luminescent center in undoped zinc oxide films deposited on silicon substrates", *Appl. Phys. Lett*. 79(7), 943-945 (2001).
9. F. S. Hickernell, "DC triode sputtered zinc oxide surface elastic wave transducers", *J. Appl. Phys*. 44(3), 1061-1071 (1973).
10. G. H. Lee, Y. Yamamoto, M. Kourogi, and M. Ohtsu, "Blue shift in room temperature photoluminescence from photo-chemical vapor deposited ZnO films", *Thin Solid Films* 386(1), 117-120 (2001).
11. A. S. Riad, S. A. Mahmoud, and A. A. Ibrahim, "Structural and DC electrical investigations of ZnO thin films prepared by spray pyrolysis technique", *Physica B* 296(4), 319-325 (2001).
12. S.-H. Lim, J. Washburn, Z. Lilientalk-Weber, and D. Shindo, "Transmission electron microscopy of threading dislocations in ZnO films grown on sapphire", *J. Vacc. Sci. Technol. A* 19(5), 2601-2603 (2001).
13. X. W. Sun and H. S. Kwok, "Optical properties of epitaxially grown zinc oxide films on sapphire by pulsed laser deposition", *J. Appl. Phys*. 86(1), 408-411 (1999).
14. H. Cao, J. Y. Wu, H. C. Ong, J. Y. Dai, and R. P. H. Chang, "Second harmonic generation in laser ablated zinc oxide thin films", *Appl. Phys. Lett*. 73(5), 572 -574 (1998).
15. J. Perriere, E. Millon, W. Seiler, C. Boulmer-Leborgne, V. Craciun, O.Albert, J. C. Loulergue, and J. Etchepare, "Comparison between ZnO films grown by femtosecond and nanosecond laser ablation", *J. Appl. Phys*. 91(2), 690-696 (2002).
16. R. E. Leuchtner, "Mass spectrometry and photoionization studies of the ablation of ZnO: Ions, neutrals, and Rydbergs", *Appl. Surf. Sci*. 12, 626-632 (1998).
17. N. Cherief, D. Givord, A. Lienard, K. Mackay, O. F. K. McGrath, J. P. Rebouillat, F. Robaut and Y. Souche "Laser ablation deposition and magnetic characterization of metallic thin films based on rare earth and transition metals", *J. Magn. Magn. Mate*. 121, 94-101 (1993).
18. S. H. Bae, S. Y. Lee, B. J. Jin, and S. Im, "Pulsed laser deposition of ZnO thin films for applications of light emission" *Appl. Surf. Sci*. 154–155, 458-461 (2000).
19. H. L. Hartnagel, A. L. Dawar, A. K. Jain, and C. Jagadish, *Semiconducting Transparent Thin Films*, Institute of Physics, London, 1995.
20. Jacques I. Pankove, *Optical process in semiconductors*, Dover publications, New York, 1975.
21. B. E. Sernelius K. F. Berggren Z. C. Jin, I. Hamberg, and C. G. Granqvist, "Band gap tailoring of ZnO by menas of heavy Al doping", *Phys. Rev. B* 37(17), 10244–10248 (1988).
22. Frederik Claeyssens, Andrew Cheesman, Simon J. Henley, and Michael N.R. Ashfold, "Studies of the plume accompanying pulsed ultraviolet laser ablation of zinc oxide", *J. Appl. Phys*. 92(11), 6886-6894 (2002).
23. A. A. Voevodin, S. J. P. Laube, S. D. Walck, J. S. Solomon, M. S. Donley, and J. S. Zabinski, "Pulsed laser deposition of diamond-like amorphous carbon films from graphite and polycarbonate targets", *J. Appl. Phys*. 78(6), 4123-4130 (1995).
24. I.Weaver, G.M.Martin, W.G.Graham, T.Morrow, and C.L.S,Lewis, "The Langmuir probe as a diagnostic of the electron component within low temperature laser ablated plasma plumes", *Rev. Sci. Instr*., 70(3) 1801-1805 (1999).
25. M. H. Hong and Y. F. Lu, "Comment on Emission of prompt electrons during excimer laser ablation of aluminum targets", *Appl. Phys. Lett* 76(2), 248(2000).
26. J.D.Swift and M.J.R.Schwar, *Electrical Probes for Plasma Diagnostics*, Iiiffe, London, 1970.
27. T.N.Hansen, J. Schou, and J.G. Lunney, "Angle-resolved energy distributions of laser ablated silver ions in vacuum", *Appl. Phys. Lett.* 72(15), 1829-1831(1998).
28. B. Toftmann, J.Schou, T.N.Hansen, and J.G.Lunney, "Angular Distribution of Electron Temperature and Density in a Laser-Ablation Plume", *Phys. Rev. Lett*., 84(17), 3998-4001 (2000).